

Article

Relationship between Visual and Thermal Comfort and Electrodermal Activity in Campus Blue–Green Spaces: A Case Study of Guangzhou, China

Xuefei Wang ¹, Zhiqi Chen ¹, Dawei Ma ², Tingting Zhou ¹, Jintang Chen ^{1,*}  and Xing Jiang ^{1,*}

¹ College of Architecture and Urban Planning, Guangzhou University, Guangzhou 510006, China; saup_wxf@gzhu.edu.cn (X.W.); chanzk9210@163.com (Z.C.); ouin6120@163.com (T.Z.)

² School of Management, Guangzhou University, Guangzhou 510006, China; madavid@gzhu.edu.cn

* Correspondence: jtchen@gzhu.edu.cn (J.C.); jiangxing@gzhu.edu.cn (X.J.); Tel.: +86-150-8805-0942 (J.C.); +86-138-2445-7736 (X.J.)

Abstract: The rapid speed of urbanization in modern cities has led to various environmental challenges impacting human activities, livelihoods, and comfort. One of these effects is the urban heat island, which describes the increase in temperature in an urban area resulting from the replacement of natural surfaces with concrete, buildings, and other structures that absorb and retain heat. Variations in individual perception and adaptive ability present additional challenges when trying to ensure outdoor comfort and require advanced measuring instruments and simulation tools to accurately predict a broad range of related variables. In this study, we investigated three different types of blue–green spaces (six in total) on the campus of Guangzhou University, focusing on their distinct layouts. The aim was to evaluate these spaces' microclimate and sunlight intensity conditions by quantifying several environmental factors. Subjective comfort assessments and objective physiological parameter measurements were conducted using questionnaires and biosensors, respectively. The results revealed the following: (1) Different types of blue–green spaces exhibit distinct microclimate and visual environment characteristics, and while similar patterns emerged, certain environmental parameters revealed important differences. (2) There is a significant association between individuals' thermal and visual comfort in blue–green spaces and multiple environmental factors. (3) Linear regression analysis demonstrated the strong predictive capabilities of skin conductance indicators (Rsc, SCR, and nSCR) in assessing individuals' outdoor visual–thermal comfort levels, with R² exceeding 0.5, indicating high accuracy. These findings provide valuable insights and references for urban planners and designers seeking to enhance the visual and thermal aspects of sustainable landscapes on campuses as well as in other outdoor environments.

Keywords: thermal comfort; visual comfort; campus blue–green space; microclimate; sunlight intensity; electrodermal activity



Citation: Wang, X.; Chen, Z.; Ma, D.; Zhou, T.; Chen, J.; Jiang, X. Relationship between Visual and Thermal Comfort and Electrodermal Activity in Campus Blue–Green Spaces: A Case Study of Guangzhou, China. *Sustainability* **2023**, *15*, 11742. <https://doi.org/10.3390/su151511742>

Academic Editor: Vincenzo Costanzo

Received: 26 June 2023

Revised: 17 July 2023

Accepted: 27 July 2023

Published: 30 July 2023



Copyright: © 2023 by the authors. Licensee MDPI, Basel, Switzerland. This article is an open access article distributed under the terms and conditions of the Creative Commons Attribution (CC BY) license (<https://creativecommons.org/licenses/by/4.0/>).

1. Introduction

With the rapid pace of urbanization, urban green and blue spaces have become essential components of the urban ecosystem, playing pivotal roles in promoting sustainable urban development and enhancing residents' physical and mental well-being [1]. However, the effectiveness and ecological benefits of these spaces are often constrained by environmental factors such as the urban heat island effect, which limit these spaces' accessibility and comfort [2]. These limitations not only decrease outdoor engagement but also hinder urban areas' overall vibrancy [3]. The fact that several elements influence personal perception and comfort levels in urban blue–green spaces further contributes to the complexity involved in addressing these issues. While early research on this topic primarily focused on examining the impact of various stimuli on individuals' environmental perceptions, more

recent studies have emphasized the thermal and visual perception aspects of environmental comfort [4–6].

Visual–thermal comfort is critical for mitigating heat stress and adapting to climate change [7]. The American Society of Heating, Refrigerating, and Air-Conditioning Engineers (ASHRAE) defines thermal comfort as ‘the psychological satisfaction of individuals with the thermal environment’ [8]. Research has shown that urban green spaces can effectively reduce ambient temperatures and enhance thermal comfort by facilitating evaporative heat dissipation and providing shade [9]. Natural water bodies have the ability to evaporate cooling air to improve the thermal environment [10]. Vision, a vital sensory component linking individuals to their surroundings, has also been shown to play a critical role in the individual perception of the external environment [11]. Visual comfort refers to the subjective sense of well-being derived from the visual environment [12], and in outdoor settings, it is determined by environmental factors such as lighting [13]. The presence of trees and vegetation in blue–green spaces can attenuate sunlight and provide shade, thereby improving people’s visual comfort, while bodies of water provide wider views and moist air [14]. Different types of blue–green spaces exhibit varying effects on visual–thermal comfort levels due to variations in the vegetation and the layout of different spaces [15].

In recent years, extensive research has underscored the comprehensive impact of visual–thermal comfort. Specifically, empirical investigations have shed light on the discernible influence of the visual environment on thermal conditions [15], as well as the potential of augmenting visual comfort to mitigate thermal discomfort [16]. Furthermore, scholarly inquiries have delved into the interdependent relationship between the thermal environment and the evaluation of the visual milieu. Notably, Lam et al. revealed a positive correlation between thermal comfort voting and visual comfort voting [6], while Lau and Choi elucidated a significant association between thermal comfort and aesthetic assessment, unveiling a robust negative correlation between thermal sensation voting (TSV) and perceptual aesthetic voting [17]. Importantly, explorations of urban landscapes and street thermal comfort have demonstrated that the presence of verdant vegetation within street spaces engenders heightened visual comfort and enhances the acceptance of the thermal environment [14,18], despite potential deviations from pleasurable experiences [19]. Moreover, previous investigations have elucidated the psychological implications of visual perception on human thermal sensation [20], yet it has been found that manipulating the visual environment does not alter thermal perception when individuals are exposed to temperatures equal to or exceeding 30 °C [21].

The interaction between humans and their environment is a complex biophysical process, and accurately evaluating human comfort levels requires quantifying physiological indicators and surveying individuals via questionnaires to account for the many physiological parameters involved [22,23]. The thermal environment influences the human body in several ways and leads to changes in physiological indicators such as skin temperature (SKT) [24], heart rate (HR) [25], electrodermal activity (EDA) [26], and respiration rate (RESP) [27]. Alterations in these indicators directly impact individuals’ subjective perceptions and change how they then respond to the environment. Visual comfort is determined by an even wider range of factors, and analyzing these non-thermal aspects requires the careful consideration of several additional factors [28]. For instance, sunlight alters the brightness and color of the outdoor environment, which affects both visual perception and mental states [29]. Exposure to intense sunlight in a hot environment often reduces visual comfort, and this change in one’s psychological state has an impact on the regulation of the body’s thermal balance, ultimately reducing thermal comfort as well. Therefore, the visual–thermal environment is defined by the interrelationships between visual–thermal and physiological responses [30].

In recent years, research has increasingly focused on investigating the relationship between subjective human comfort and objective physiological indicators to evaluate environmental comfort [31]. One particular indicator that has received considerable attention

is skin temperature (SKT) due to its sensitivity to changes in ambient temperature and its strong correlation with thermal sensation votes (TSV) and thermal comfort votes (TCV) [32]. Skin conductance response (SCR), a highly sensitive measurement method, has frequently been used to discern variations in human responses to several kinds of environmental stimuli [33,34]. In this study, we aimed to improve the degree of accuracy achieved when predicting changes in visual–thermal comfort and electrodermal activity (EDA) by analyzing variations in participants’ visual–thermal comfort levels across six campus blue–green spaces. Specifically, we sought to address the following research questions (Table 1).

Table 1. Information about the six campus spaces.

Research Question	
Q1	Do microclimate and visual environmental factors vary according to identifiable patterns and feature significant differences in different spaces? How do these factors affect individuals’ thermal and visual comfort levels?
Q2	Is there a correlation between thermal comfort and visual comfort in outdoor green spaces?
Q3	Can skin conductance response serve as an effective predictor of visual–thermal comfort?

2. Materials and Methods

2.1. Study Areas and Sample Selection

This study was conducted at a university in Guangzhou, an area in southern China where the weather is typically hot and humid. According to the Köppen climate classification, which is widely used in ecology and climatology, Guangzhou belongs to a humid subtropical zone (Cfa) and is characterized by a subtropical monsoon marine climate [35]. Climatological data from the China Meteorological Administration, shown below, spans the period from 1991 to 2020 (Figure 1).

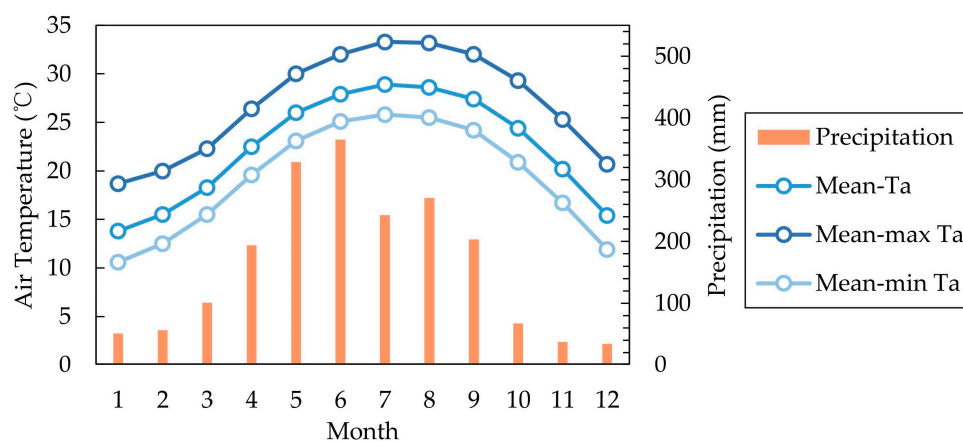


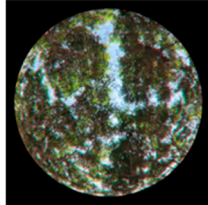
Figure 1. Monthly mean/maximum/minimum air temperature and precipitation in Guangzhou from 1991 to 2020.

Based on climatological data, Guangzhou experiences its highest average air temperature in July, reaching 28.9 °C, with an average maximum temperature peaking at 33.3 °C. Conversely, January has the lowest monthly mean air temperature, averaging 13.8 °C, with an average minimum temperature of 10.6 °C. The average monthly rainfall in Guangzhou is recorded as 162.6 mm.

The university campus is in Guangzhou’s Panyu District and covers an area of approximately 125.33 hectares. Three criteria, sky view factor (SVF), the intended purposes of the area, and typology [36], formed the basis for selecting three distinct types of outdoor spaces on the campus, which we describe as tree-linear, open, and semi-open. Each of these spaces feature diverse landscape elements that draw on features of blue–green spaces in varying proportions and exhibit a variety of seasonal changes, providing a rich array of

visual effects. Ultimately, each space that was chosen was determined to represent a typical type of space found on campus (Table 2).

Table 2. Information about the six campus spaces.

Space Types	Scene Descriptions	Spatial Characteristics	Scene Photo	Fish-Eye Photo	SVF
Tree–Linear Space	The terrain is relatively flat, with ground material comprising primarily permeable pavement. Vegetation includes tall trees and ground-covered plants.	A1 Adjacent to the river but not in sight; high enclosure level; dominated by tall trees.			0.284
		A2 Adjacent to a natural river; low enclosure level; dominated by tall trees and shrubs.			0.440
Open Space	The terrain is relatively flat, with ground material comprising primarily impermeable pavement. Tall trees and aquatic plants dominate the vegetation.	B1 Adjacent to an artificial lake; dominated by tall and large trees.			0.952
		B2 Adjacent to a natural river; dominated by short shrubs and grasses.			0.934
Semi–Open Space	The terrain is relatively flat, with ground material comprising primarily impermeable pavement. Vegetation includes tall trees and shrubs.	C1 Not adjacent to the river; dominated by short, grassy trees.			0.514
		C2 Adjacent to the river but not in sight; dominated by tall and large trees.			0.325

2.2. Microclimate and Sunlight Intensity

The thermal environment comprises several important elements, including air temperature (T_a), relative humidity (R_h), wind speed (W_s), moving wind speed (M_w), and globe temperature (T_g). These factors, along with sunlight intensity (SI), collectively influence individual perception of the outdoor space environment [37]. In our monitoring activities, we referred to the ISO 7726 standard [38], which presents comprehensive methodologies for the measurement of temperature, humidity, wind speed, and thermal radiation.

Moreover, we have followed the guidance outlined in ISO 7243 [37], a widely recognized standard specifically designed for the assessment of thermal comfort in outdoor settings. Concerning the measurement of outdoor illuminance, it is recommended to adhere to the national standard GB/T 5700-2008 [39] “Methods for Measurement and Reporting of Environmental Photometry”.

Based on the climate data derived from the China Meteorological Administration spanning the period 1991–2020, the monthly mean temperatures and precipitation levels observed during the summer months of June to September were comparatively lower. The existing scientific literature suggests that participants’ thermal perception remains unchanged even with adjustments made to the visual environment, when exposed to environmental conditions ≥ 30 °C [16,40]. Therefore, for the purpose of our study, we chose 25 October 2022 as the date for field measurements, during which the ambient temperature ranged between 17 °C and 30 °C. The measuring instruments were securely positioned at designated points within each space at 1.5 m above the ground to ensure that relevant climate parameters were accurately captured. The experiment was conducted from 12:30 to 17:30 on the same day, with recordings taken once per minute in each of the six spaces. The results, including valid measurement ranges and the accuracy of each parameter, are presented in Table 3.

Table 3. Measurement parameters and device specifications.

Instrument	Parameter	Valid Range	Accuracy
Kestrel/ weather station NK-5500	Wind speed	0~5 m/s	± 0.05 m/s
ONSET/HOBO Pro U23-002	Air temperature Relative humidity	−40~70 °C 0~100%	± 0.5 °C $\pm 2.5\%$
WBGT temperature index meter JTR-04	Globe temperature	5~120 °C	± 0.5 °C
Multi-probe illuminometer ZDS-10F-2D	Sunlight intensity	0–20 $\times 10^4$ klx	$\pm 4\%$

2.3. Questionnaire Survey and Physiological Testing

2.3.1. Participants

A total of 20 student volunteers (10 males and 10 females) participated in the study. The participants’ ages ranged from 18 to 22 years, with heights and weights spanning from 1.55 m to 1.85 m and from 50 kg to 80 kg, respectively (Table 4). All participants were students who had lived in Guangzhou for more than one year, which was determined to be an adequate amount of time to acclimate to local climatic conditions and accurately perceive temperature changes. Before the experiment, each participant received a detailed briefing on the experimental procedure, requirements, and precautions. All participants had normal vision and were deemed capable of providing reliable assessments of their visual environment.

Table 4. Summary of participants’ information (values are means \pm standard deviation).

Gender	Number	Age (Years)	Height (cm)	Weight (kg)	BMI (kg/m ²)
Male	10	18.8 \pm 0.98	175.10 \pm 5.11	68.75 \pm 8.60	22.37 \pm 2.22
Female	10	19.2 \pm 0.87	163.60 \pm 6.34	55.40 \pm 9.05	20.62 \pm 2.63
Total	20	19 \pm 0.95	169.35 \pm 8.14	62.08 \pm 11.07	21.50 \pm 2.58

Participants were required to adhere to a specific dress code, which included wearing underwear, a short-sleeved shirt, sports pants, cotton socks, and sports shoes, resulting in a total clothing insulation value of approximately 0.5 clo [41]. Additionally, participants were

informed to avoid staying up late and consuming alcohol the day prior to the experiment, ensuring their physical and mental well-being during the test.

Prior to the experiment, each participant received a comprehensive briefing on the experimental procedure, requirements, and precautions. All participants had normal vision and were deemed capable of providing reliable assessments of their visual environment. To maintain consistent environmental stimuli and optimize visual clarity, the use of sun umbrellas was prohibited during the experiment.

2.3.2. Experimental Design

Participants were divided into five groups, with each group consisting of four members. All groups were balanced in terms of gender, and their members had similar physical characteristics. A one-hour interval separated experiments with the participants of each group. Prior to the start of an experiment, participants were instructed to rest in a shaded area for 10 min to stabilize their physiological state. During this time, an experimental assistant helped the participants attach the physiological monitoring devices. Under the assistant’s guidance, participants were instructed to walk in each designated space and observe the surrounding landscape for 5 min. Once the participants had adapted to a given environment, their physiological response was measured via specified parameters. Participants then completed thermal perception and visual perception questionnaires. This process was repeated until all participants had experienced every designated space (Figure 2).

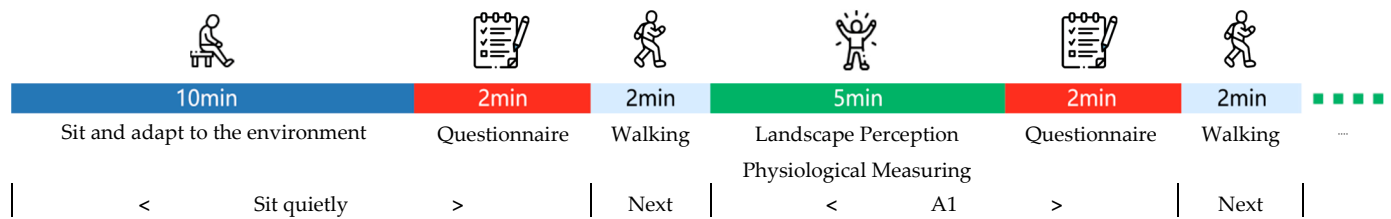


Figure 2. Experimental procedure.

2.3.3. Questionnaire Design

The questionnaire used in this study consisted of three sections: the initial section collected the participants’ personal information, and the second and third parts contained assessments of subjective thermal comfort and subjective visual comfort according to the definitions provided by ASHRAE [8]. These assessments employed a Likert scale in which participants rated their thermal and visual sensation level on a scale of one to five and their visual and thermal comfort level on a scale of one to seven. Their responses corresponded to the following physiological parameters: thermal sensation vote (TSV), thermal preference vote (TPV), thermal comfort vote (TCV), wind sensation vote (WSV), humidity sensation vote (HSV), solar radiation sensation vote (RSV), sunlight sensation vote (SSV), sunlight preference vote (SPV), and visual comfort vote (VCV) (Table 5).

Table 5. Questionnaire design.

Section 1: Participant Information			
Name:	Height:		
Gender:	Weight:		
Age:	BMI:		
Section 2: Thermal Comfort Evaluation			
Q1: Thermal Sensation	Cold	−3 −2 −1 0 1 2 3	Hot
Q2: Humidity Sensation	Dry	−3 −2 −1 0 1 2 3	Humid

Table 5. *Cont.*

Q3: Wind Speed Sensation	Low	−3 −2 −1 0 1 2 3	High
Q4: Solar Radiation Sensation	Weak	−3 −2 −1 0 1 2 3	Strong
Q5: Thermal Comfort	Uncomfortable	0 1 2 3 4	Comfortable
Q6: Thermal Preference	Cooler	−1 Unchanged 0 Warmer 1	
Section 3: Visual Comfort Evaluation			
Q1: Sunlight Sensation	Dim	−3 −2 −1 0 1 2 3	Bright
Q2: Visual Comfort	Uncomfortable	0 1 2 3 4	Comfortable
Q3: Sunlight Preference	Darker	−1 Unchanged 0 Brighter 1	

2.3.4. Physiological Measurement

ErgoLAB, a physiological monitoring instrument, which is specifically designed for outdoor environments and capable of detecting subtle environmental changes via sensors, was used to measure participants' electrodermal activity (EDA) in real time. Data recording and analysis were then performed using the ErgoLAB HMI Assessment System. The measurement range and accuracy of the monitoring instrument for skin conductance response (SCR) is presented in Table 6.

Table 6. Measurement parameters and specifications of the device.

Instrument	Parameter	Valid Range	Accuracy
EDA Skin Conductance Sensor	Skin Conductance Response	0–30 μ S	0.01 μ S

Electrodermal activity (EDA) is considered the most effective and sensitive physiological parameter reflecting excitatory changes in the human sympathetic nervous system. It offers additional advantages such as stability, ease of collection, and high sensitivity [33]. This study analyzed the results of the EDA measurements according to the primary indicators of skin conductance (SC), skin conductance response (SCR), and the number of skin conductance responses (nSCR) [42]. SC refers to the contraction or relaxation of the blood vessels when the body is subjected to sensory stimulation or emotional changes, which causes changes in skin resistance due to sweat gland secretion [43]. To account for individual variation in physiological signaling, the skin conductance rate (Rsc) was used as the SC research index. Participants' average skin conductance when presented with different visual stimuli (Asc) associated with the particular visual scene, as well as their average skin conductance under sedation (Aclam), were recorded. These indices were then used to calculate the Rsc as follows [44]:

$$Rsc = \frac{Asc - Aclam}{Aclam} \quad (1)$$

SCR refers to the physiological and psychological activation state induced by stimulation and reflects short-term brain processes. The SCR amplitude reflects the intensity of both internal and external stimulation, with higher values indicating a more vigorous response [45]. The nSCR represents the number of SCRs occurrences following a stimulus event. A higher nSCR value indicates a stronger response to the stimulus.

During the experiment, the sensor was consistently placed on the right wrist of each participant, while the sensor patch was attached to the first joint of their index and middle fingers [46]. After entering a space, participants were given 2 min to adapt to climatic conditions in the surrounding environment before their EDA was recorded. This study had a particular interest in accounting for deviations in physiological index values from medical reference values; therefore, there was a pronounced focus on variations in this area.

2.3.5. Statistical Analysis

To examine the relationships between variables, SPSS 25.0 was utilized to perform a statistical analysis, with $p < 0.05$ considered to be statistically significant. Descriptive analysis, one-way analysis of variance (ANOVA), the Pearson correlation, the chi-square independence test, and linear regression were also used (Figure 3).

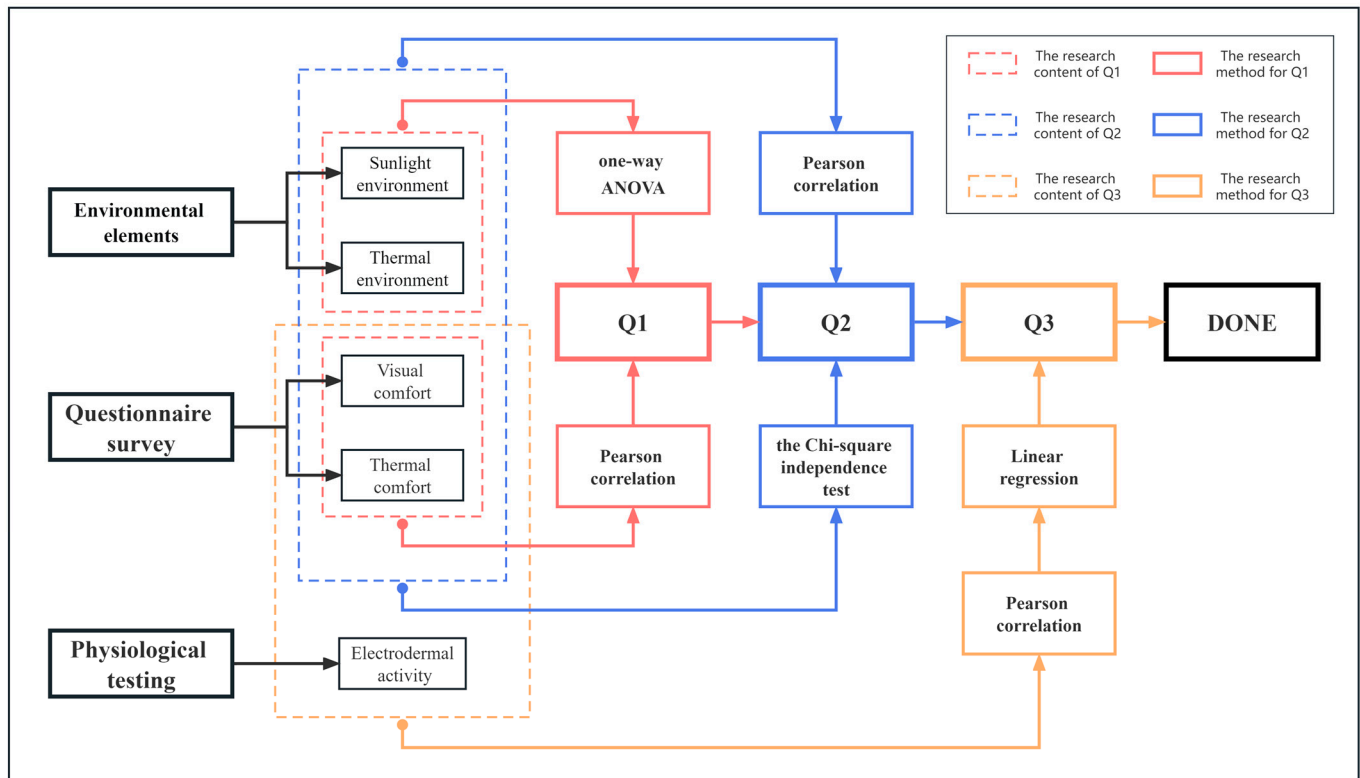


Figure 3. Methodology flow chart.

To address the first research question posed earlier, a one-way ANOVA was conducted to compare microclimate factors in different spaces to determine if there were significant differences among them. The Pearson correlation was also used to explore potential associations between thermal comfort voting and visual comfort voting within each space, as well as any possible relationships between these voting results and microclimate parameters.

For the second research question, the Pearson correlation was used to investigate the correlation between thermal and visual comfort indices and various environmental parameters. Chi-square independence tests were also performed to identify whether there was a significant association between thermal comfort measures (e.g., TSV, TPV, and TCV) and visual comfort measures (e.g., SSV, SPV, and VCV).

Regarding the third research question, we again employed the Pearson correlation to examine the relationships between physiological, microclimate, and sunlight factors. Subsequently, linear regression was performed to compare physiological parameters with the TSV and SSV, allowing us to evaluate the predictive power of physiological parameters for visual–thermal comfort.

3. Results

3.1. Variations in Microclimate and Illumination in Different Thermal Environments

Table 7 displays the mean values of the meteorological variables measured within the six spaces during the experiment. These data were processed using RayMan 1.2 to calculate the mean radiation temperature (T_{mrt}) and the universal thermal climate index (UTCI) [47]. Our findings revealed that elements in different spaces had distinct impacts

on thermal comfort, and the interplay between thermal and non-thermal factors influenced individuals' sense of comfort. Thermal factors included thermal environment indices such as T_a , R_h , W_s , T_g , and T_{mrt} , while non-thermal factors mainly involved indices related to the visual environment, such as SI . Throughout the experiment, environmental parameters exhibited variations across the six spaces, while similar patterns of change were observed across spaces of the same type (Figure 4).

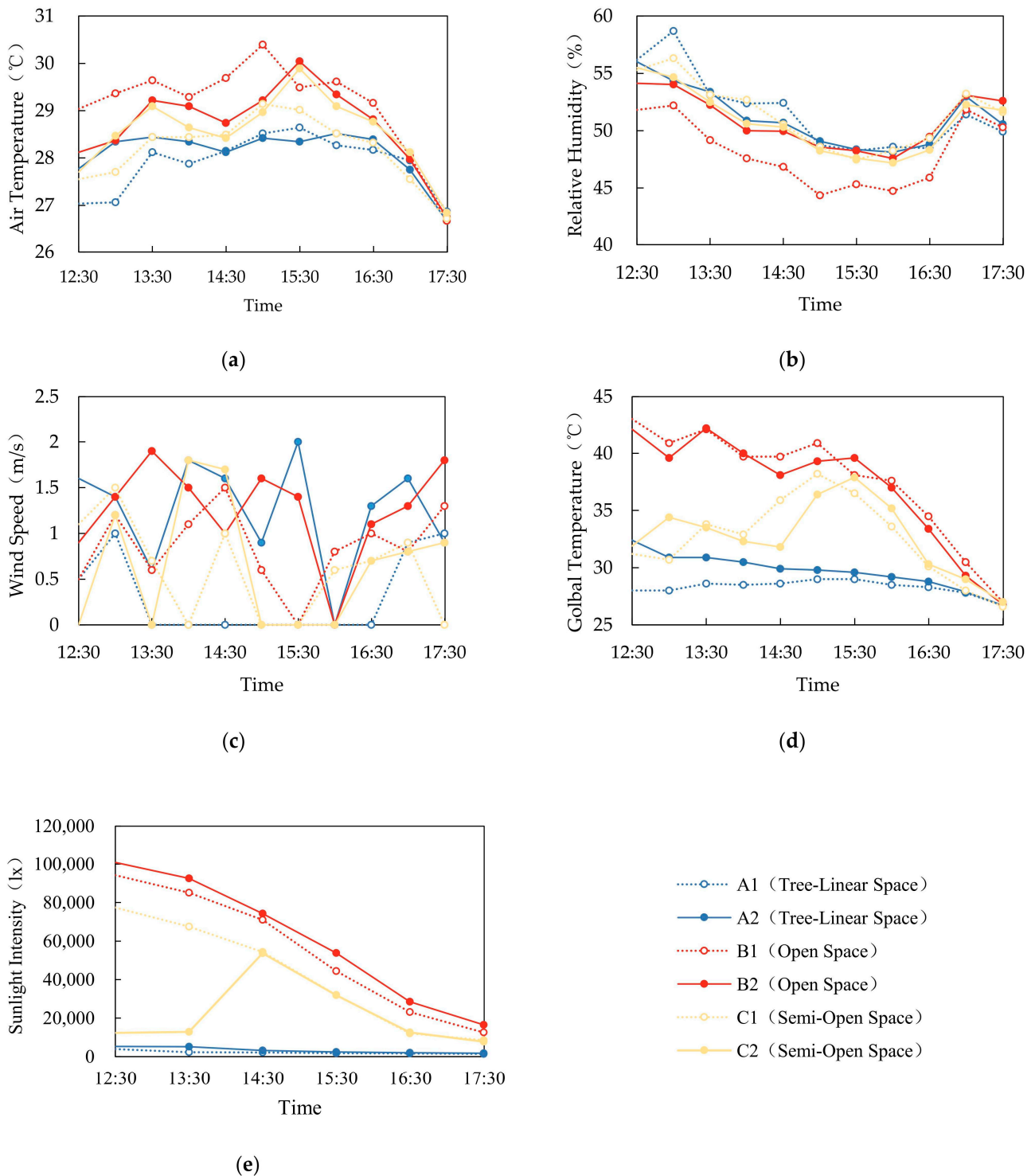


Figure 4. Variation trends of (a) air temperature, (b) relative humidity, (c) wind speed, (d) globe temperature index, and (e) sunlight intensity in six spaces.

Table 7. Mean values of environmental parameters at each measurement point.

Parameter	Tree-Linear Space		Open Space		Semi-Open Space	
	A1	A2	B1	B2	C1	C2
SVF (%)	0.284	0.440	0.952	0.934	0.514	0.325
Ta (°C)	27.91	28.21	29.39	28.91	28.38	28.68
Rh (%)	51.41	50.98	47.91	50.16	51.37	50.48
Ws (m/s)	0.43	0.93	0.82	1.02	0.52	0.56
Mws (m/s)	0.58	0.68	0.66	0.60	0.57	0.48
Tg (°C)	28.33	29.77	38.15	37.31	32.87	33.00
Tmrt (°C)	28.23	30.05	39.85	39.09	33.43	33.55
UTCI (°C)	27.40	27.80	35.20	33.70	31.00	28.55
SI (lx)	2348.40	3629.20	63,592.00	69,988.00	38,162.80	23,734.40

We conducted a one-way ANOVA to assess the variations among these environmental parameters, revealing significant differences between them ($p < 0.01$). By comparing spaces with similar SVF values (A1 and C2, A2 and C1, and B1 and B2), we were able to identify several notable features. For instance, spaces with higher vegetation coverage (A1 and C1) had lower Ta and higher Rh values. Spaces closer to water (A2 and C2) exhibited higher Ws and a lower UTCI. B1 and B2, characterized by expansive vistas, were found to have significantly higher Ws than the other spaces. In addition, B1 had the highest SVF, Ta, and Tg values and was second only to B2 in the amount of SI. At the same time, B1 had the lowest Rh, resulting in the highest UTCI. In contrast, A1 had the lowest SVF, Ta, Tg, and SI, but the highest Rh, and exhibited the lowest UTCI. These differences are believed to be the result of variations in vegetation planting patterns and distinct spatial layouts.

3.2. Correlation Analysis between Thermal Comfort and Visual Comfort

3.2.1. Changes in Visual–Thermal Comfort in Different Thermal Environments

Tables 8 and 9 present the thermal comfort and visual comfort vote results, along with their corresponding correlation coefficients. The following analysis examines variations and similarities in vote scores across different types of spaces (Figure 5).

Table 8. The voting results of visual–thermal comfort indicators across different spaces.

	A1	A2	B1	B2	C1	C2
TSV	0.20 ± 0.93	0.75 ± 0.70	1.40 ± 0.80	1.45 ± 0.59	0.75 ± 0.70	0.80 ± 0.75
TPV	2.35 ± 0.48	2.05 ± 0.50	1.95 ± 0.50	1.90 ± 0.54	2.05 ± 0.38	2.20 ± 0.40
TCV	2.90 ± 0.62	2.55 ± 0.80	1.55 ± 0.80	1.70 ± 0.90	2.35 ± 0.57	2.15 ± 0.73
HSV	0.15 ± 1.01	0.15 ± 1.01	−0.25 ± 1.26	−0.20 ± 1.36	0.05 ± 1.07	0.15 ± 1.06
WSV	0.50 ± 0.92	−0.15 ± 1.31	0.30 ± 1.27	−0.05 ± 1.32	0.15 ± 1.24	−0.20 ± 1.08
RSV	0.50 ± 1.07	1.20 ± 0.60	1.95 ± 0.97	2.00 ± 0.63	0.85 ± 0.79	0.75 ± 1.04
SSV	0.40 ± 1.02	1.40 ± 0.66	2.10 ± 1.04	2.25 ± 0.70	0.70 ± 0.95	0.90 ± 1.09
SPV	2.50 ± 0.74	2.45 ± 0.74	2.10 ± 0.62	2.05 ± 0.59	2.30 ± 0.56	2.30 ± 0.56
VCV	2.65 ± 0.57	2.45 ± 0.50	1.75 ± 0.70	1.70 ± 0.71	2.35 ± 0.57	2.15 ± 0.65

Table 9. Correlation analysis of the voting results for visual–thermal comfort.

	TSV	TPV	TCV	HSV	WSV	RSV	SSV	SPV	VCV
TSV	1								
TPV	−0.390 **	1							
TCV	−0.606 **	0.249 **	1						
HSV	−0.250 **	0.146	0.343 **	1					
WSV	−0.337 **	0.194 *	0.446 **	0.325 **	1				
RSV	0.623 **	−0.227 *	−0.487 **	−0.174	−0.255 **	1			
SSV	0.615 **	−0.189 *	−0.498 **	−0.246 **	−0.213 *	0.884 **	1		
SPV	−0.282 **	0.260 **	0.218 *	−0.091	0.019	−0.133	−0.173	1	
VCV	−0.428 **	0.242 **	0.672 **	0.413 **	0.191 *	−0.460 **	−0.475 **	0.248 **	1

Note: ** Correlation is significant at the 0.01 level (2-tailed); * correlation is significant at the 0.05 level (2-tailed).

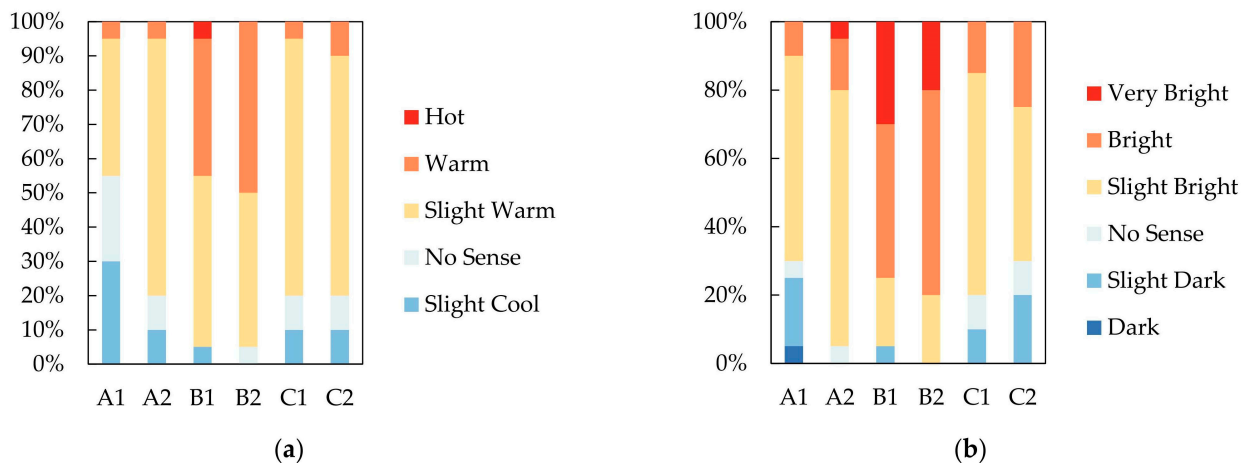


Figure 5. The proportions of thermal sensation voting (a) and sunlight sensation voting (b) across different spaces.

Regarding the TSV and SSV, the highest values can be found in B2: 1.45 (indicating a sensation between ‘warm’ and ‘relatively hot’) and 2.25 (indicating a brightness between ‘bright’ and ‘very bright’), respectively. Conversely, A1 has the lowest TSV and SSV values at 0.20 (between ‘no sensation’ and ‘relatively hot’) and 0.40 (between ‘no sensation’ and ‘dark’), respectively. The Pearson correlation revealed a significant positive correlation between the TSV and SSV, with a coefficient of 0.615. However, the TSV and SSV are negatively correlated with the TPV, TCV, HSV, WSV, SPV, and VCV but positively correlated with the RSV.

Regarding the TCV and VCV, A1 has the highest scores, while B1 and B2 have the lowest scores at 1.55 (between ‘no feeling’ and ‘less comfortable’) and 1.70 (between ‘no feeling’ and ‘less comfortable’), respectively. A significant positive correlation exists between the TCV and VCV, with a coefficient of 0.672. Additionally, the TCV and VCV show significant positive correlations with the HSV, WSV, and SPV while showing significant negative correlations with the TSV, RSV, and SSV.

3.2.2. Correlation Analysis between Visual–Thermal Comfort Index and Environmental Parameters in Different Thermal Environments

We further analyzed the correlation between thermal comfort, visual comfort, and various environmental parameters. The results revealed significant correlations between thermal comfort and environmental parameters. As shown in Table 10, both the TSV and SSV show significant positive correlations with T_a , W_s , M_w_s , T_g , T_{mrt} , the UTCI, SI, and SVF and are negatively correlated with R_h . T_{mrt} has the strongest correlation with the TSV and SSV, with correlation coefficients of 0.502 and 0.615, respectively. However, their correlation with M_w_s is relatively weak, with correlation coefficients of 0.023 and 0.330 for the TSV and SSV, respectively. No significant correlation was observed between W_s and the TSV or SSV. This is likely due to the low efficiency of air heat exchange in low W_s environments, resulting in heat accumulation that leads to the feeling of stuffiness.

Table 10. Correlation analysis between visual–thermal comfort voting and microclimate elements.

	T_a	R_h	W_s	M_w_s	T_g	T_{mrt}	UTCI	SI	SVF
TSV	0.164	−0.006	0.068	0.023	0.288 **	0.300 **	0.332 **	0.308 **	0.265 **
TPV	−0.155	0.071	−0.118	−0.131	−0.166	−0.164	−0.249 **	−0.206 *	−0.270 **
TCV	−0.564 **	0.258 **	0.102	−0.225 *	−0.615 **	−0.622 **	−0.482 **	−0.565 **	−0.469 **
SSV	0.562 **	−0.340 **	−0.012	0.330 **	0.615 **	0.615 **	0.478 **	0.478 **	0.533 **
SPV	−0.118	−0.154	−0.021	−0.046	−0.239 **	−0.242 **	−0.233 *	−0.257 **	−0.227 *
VCV	−0.251 **	0.048	0.136	−0.066	−0.392 **	−0.387 **	−0.317 **	−0.399 **	−0.223 **

Note: ** Correlation is significant at the 0.01 level (2-tailed); * correlation is significant at the 0.05 level (2-tailed).

Furthermore, significant correlations were observed between the TCV and VCV and environmental parameters. The TCV and VCV show significant negative correlations with T_a , GT , T_{mrt} , the UTCI, SI , and SVF while showing a significant positive correlation with R_h . Specifically, T_{mrt} exhibits the strongest correlation with the TCV, with a correlation coefficient of -0.622 , while SI has the strongest correlation with the VCV, with a correlation coefficient of -0.565 . Just as with the TSV and SSV, we found no significant correlations between W_s and the TCV or VCV.

3.2.3. Correlation Analysis of Visual–Thermal Comfort

Figure 6 depicts the results of the linear regression analysis examining the relationship between thermal sensation and light sensation voting in response to a 1°C change in the UTCI and a 1 K lux increase in light intensity. These parameters were factored into our analysis in line with prior research, and a strong positive correlation between the two variables emerged [48]. This confirms that individuals tend to perceive their environment as brighter when they experience a higher degree of thermal sensation.

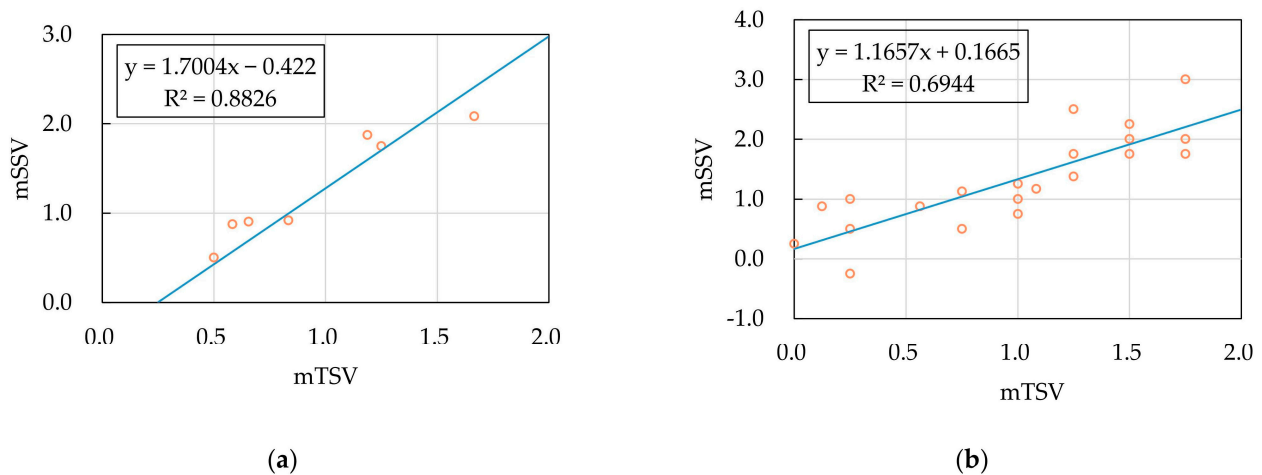


Figure 6. Linear regression of mean TSV (mTSV) and mean SSV (mSSV) based on 1°C UTCI (a) and 1 K lux (b). $p < 0.01$ (double tail).

The TSV exhibited significant correlations with the SSV, SPV, and VCV, with chi-square values of 87.347, 17.718, and 59.088 and DF values of 20, 8, and 12, respectively (Figure 7a–c). These findings suggest that, as individuals experience higher temperatures, they tend to perceive their environment as visually brighter, further confirming the association between temperature and light perception. The results also reveal that individuals prefer darker lighting in warmer environments and brighter lighting in more temperate environments, indicating that light preference is influenced by temperature. Moreover, it was observed that individuals not only experience thermal discomfort in hot environments but also experience visual discomfort, suggesting an additional relationship between visual comfort and temperature.

Significant correlations were also observed between the TPV and SSV, the SPV, and the VCV, with chi-square values of 18.729, 39.251, and 16.059 and DF values of 10, 10, and 6, respectively (Figure 7d–f). The data analysis results indicated that different lighting conditions led to variations in individuals' temperature preferences, suggesting that light perception plays a role in determining temperature preference. Furthermore, light preference and visual comfort affect how individuals evaluate their thermal comfort, indicating a reciprocal relationship between light preference, visual comfort, and temperature.

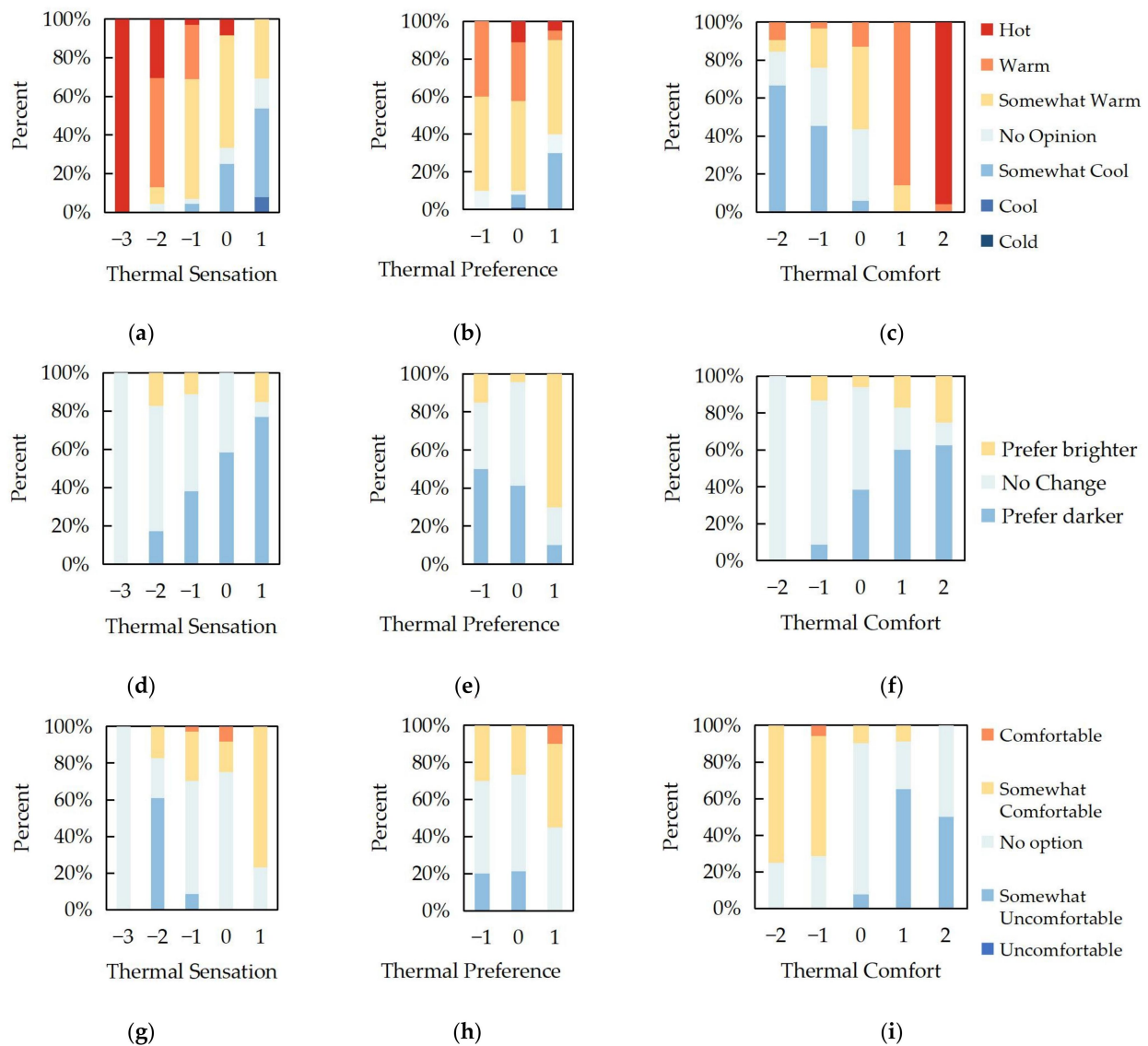


Figure 7. (a,d,g) are percentage bar charts for TSV and SSV, SPV, and VCV, respectively. (b,e,h) correspond to the percentage bar charts for TPV and SSV, SPV, and VCV, respectively. (c,f,i) display percentage bar charts for TCV and SSV, SPV, and VCV, respectively.

Moreover, the TCV showed significant correlations with the SSV, SPV, and VCV, with chi-square values of 95.224, 34.250, and 119.065 and DF values of 50, 20, and 30, respectively (Figure 7g–i). An in-depth analysis of the relationship between the TSV, SSV, TPV, and VCV revealed that different lighting conditions affect individuals' sensations and their evaluation of thermal comfort, and lighting preference also influences individuals' evaluation of thermal comfort. These findings suggest that light perception significantly impacts thermal comfort and that visual comfort is thus correlated with thermal comfort.

3.3. Correlation Analysis between Physiological Parameters and Thermal Comfort

3.3.1. Changes in Physiological Parameters in Different Types of Spaces

Table 11 presents an overview of the average changes in physiological parameters among the participants in each space during the experiment, with the Rsc, SCR, and nSCR used as indices to account for individual variations in physiological signals. As can be seen, B1 is the space with the highest average Rsc (0.641), while A1 has the lowest (0.286). The maximum SCR amplitude can be seen in B1 (0.43), while the minimum is found in A2 (0.32). The highest nSCR value occurs in A1 (44.950), while the lowest occurs in B2 (28.950).

Table 11. Mean values of different skin electrical indices in each space.

EDA	A1	A2	B1	B2	C1	C2
Rsc	0.286	0.336	0.641	0.456	0.489	0.623
SCR	0.40	0.33	0.43	0.37	0.39	0.37
nSCR	44.950	39.150	33.150	28.950	42.900	38.611

A one-way ANOVA was performed for the indices in each space. The results revealed significant differences in the Rsc and nSCR among the six spaces ($p < 0.05$), but no significant differences in SCR were identified ($p > 0.05$). Subsequently, Tukey's Honestly Significant Difference (HSD) was conducted to further confirm whether there were significant differences between spaces (Figure 8a–c).

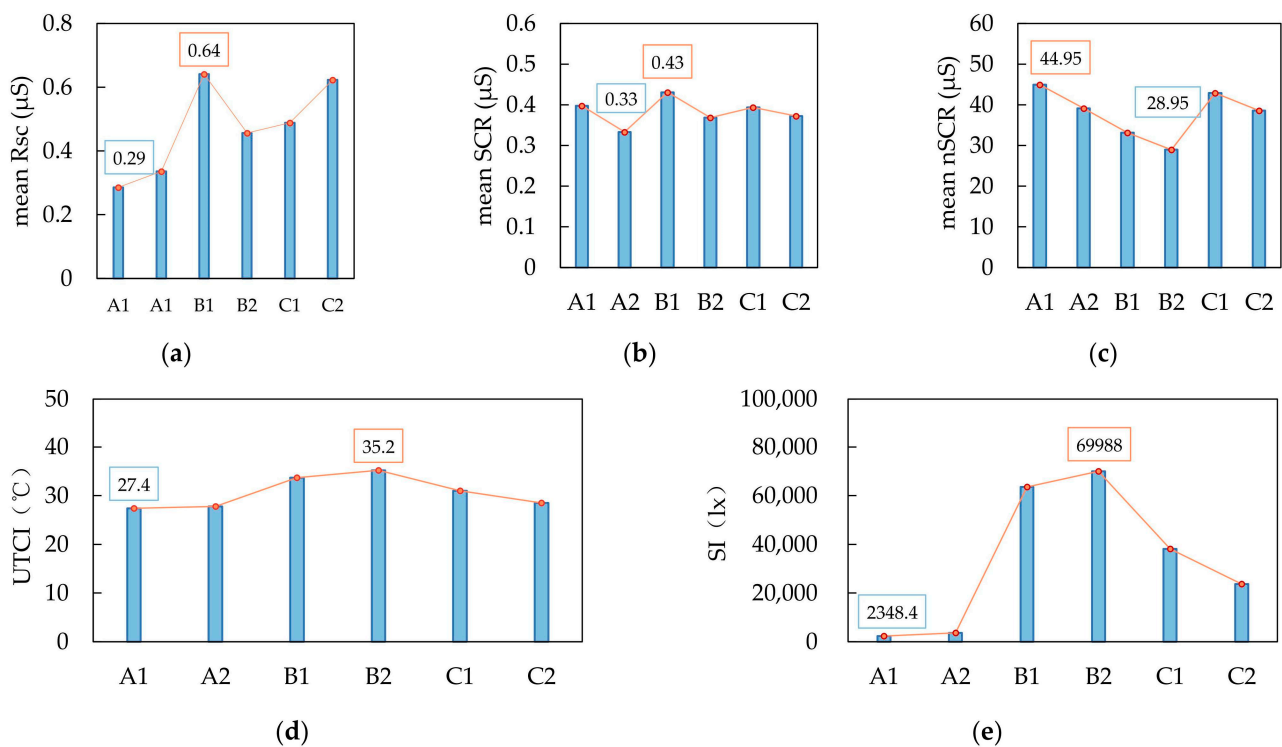


Figure 8. (a–c) represent the mean Rsc, SCR, and nSCR, respectively, while (d,e) represent UTCI and SI, respectively, for the six spaces.

Figure 8d,e illustrate variations in the mean UTCI and SI values across different spaces. It can be seen that the UTCI follows a pattern similar to SCR and the Rsc but exhibits an opposite trend when compared to the nSCR. Similarly, SI closely aligns with SCR but runs counter to the nSCR.

3.3.2. Correlation Analysis between Physiological Parameters and Environmental Parameters under Different Spatial Conditions

We conducted a correlation analysis between each skin conductance index and the environmental parameters. The results, shown in Table 12, show positive correlations between the Rsc index and T_a , T_g , T_{mrt} , the UTCI, and SI, with correlation coefficients of 0.194, 0.214, 0.223, 0.192, and 0.246, respectively. On the other hand, the nSCR index is negatively correlated with T_a , M_{ws} , T_g , T_{mrt} , the UTCI, SI, and SVF, with correlation coefficients of -0.400 , -0.238 , -0.382 , -0.379 , -0.267 , -0.297 , and -0.300 , respectively. In addition, the nSCR is positively correlated with Rh, with a correlation coefficient of 0.301. However, no significant correlations were found between SCR and environmental parameters, and the observed spatial differences were minimal, perhaps limited by individual or

other spatial variations. Nonetheless, the results suggest that changes in SCR can serve as a supplementary index for assessing comfort, providing insights into the human body’s physiological response to the thermal environment.

Table 12. Correlation analysis between skin electric parameters and environmental parameters.

EDA	Ta	Rh	Ws	Mws	Tg	Tmrt	UTCI	SI	SVF
Rsc	0.194 *	−0.106	−0.063	0.020	0.214 *	0.223 *	0.192 *	0.246 **	0.138
SCR	−0.020	0.110	0.059	0.058	0.046	−0.148	0.014	0.064	0.071
nSCR	−0.400 **	0.301 **	−0.044	−0.238 **	−0.382 **	−0.379 **	−0.267 **	−0.297 **	−0.300 **

Note: ** Correlation is significant at the 0.01 level (2-tailed); * correlation is significant at the 0.05 level (2-tailed).

3.3.3. Relationship between Physiological Parameters and Apparent Thermal Comfort

Figure 9 delineates the linear regression associations among the EDA index, TSV, and SSV, treating voting values exceeding 3 as an indication of minimal personal factor influence.

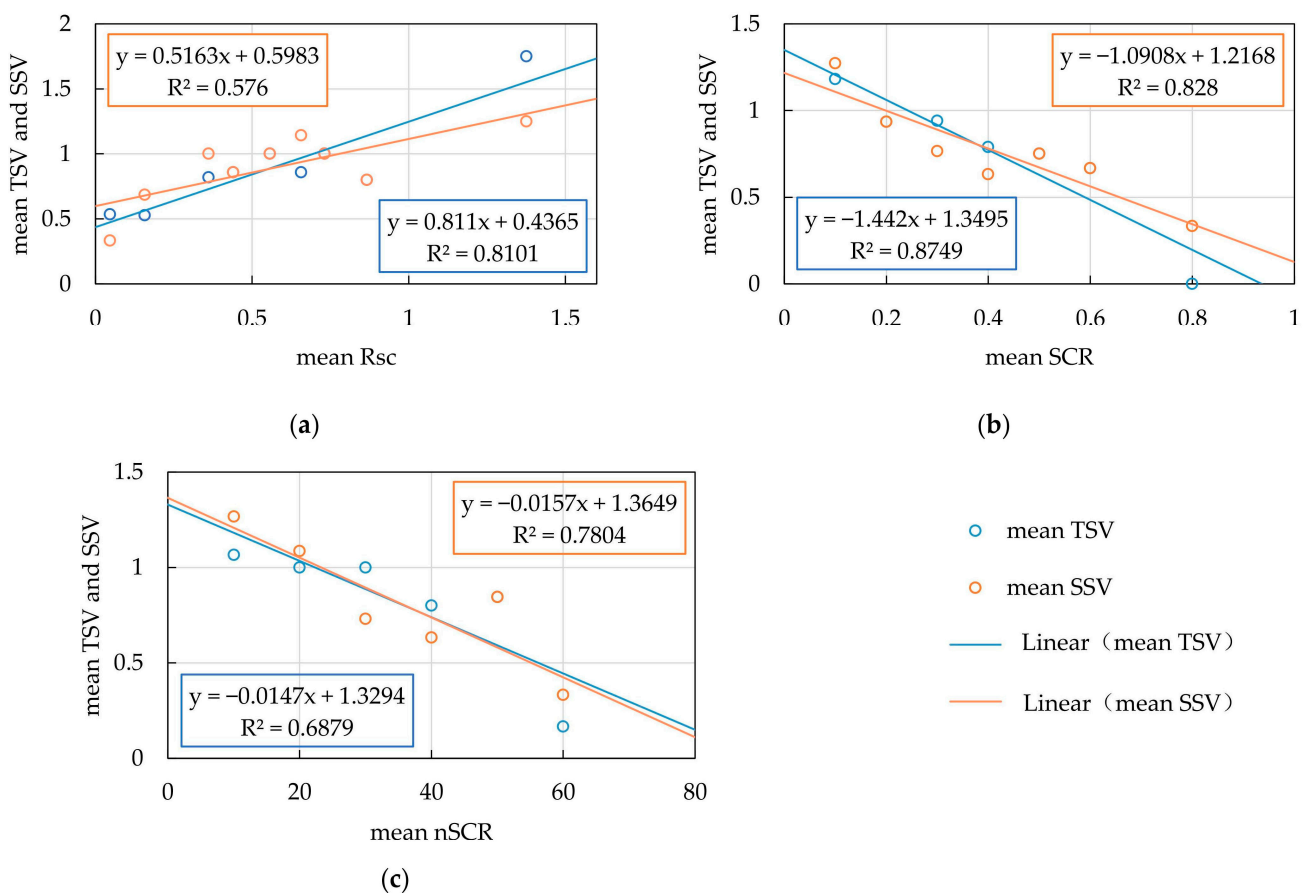


Figure 9. (a–c) show linear regression relationships of mean Rsc, SCR, nSCR, mean TSV (mTSV), and mean SSV (mSSV), respectively.

4. Discussion

By comparing data from measurement points in six unique spaces, significant differences were identified among environmental parameters in different types of spaces. Among these parameters, Ta and SI were found to be the most affected. When comparing spaces of the same type, it was revealed that spaces with dense vegetation and proximity to water produced more comfortable environmental conditions than spaces with sparse vegetation and high canopy cover (A2, B2, and C2). The SVF values for space A2, B2, and C2 were 0.440, 0.934, and 0.325, respectively. The mean Ta was recorded as 28.6 °C, with

a relative humidity of 50.54%. Spaces with dense vegetation and adjacent water sources benefited from cooling and humidifying effects, while areas with sparse vegetation and high canopy cover had higher T_a and lower R_h , reducing comfort levels.

In addition, a positive correlation was identified between the TSV and SSV: the correlation coefficient was 0.615, implicating thermal and non-thermal factors. However, the combined effect of these factors varied across different space types, resulting in differences in UTCI values. Previous studies have established the significant impact of the UTCI on individuals' subjective TSV; this study found that the UTCI also influences the SSV. In spaces characterized by high T_a , the UTCI variations had a more pronounced impact on the TSV and TCV, with individuals tending to experience more comfortable thermal sensations in low SI environments. In spaces with low T_a , the TSV increased with an increase in SI.

This study also explored the relationship between UTCI levels and visual comfort. Under conditions of low outdoor light intensity, higher UTCI levels were observed to reduce individuals' SSV and increase the VCV. In contrast, environments with higher SI resulted in lower UTCI levels, suggesting a more comfortable visual experience.

Furthermore, three physiological indices (Rsc, SCR, and nSCR) were identified as being particularly sensitive to environmental changes in outdoor environments, and both thermal and non-thermal factors were significantly correlated with the Rsc and nSCR. The correlation coefficients with T_g were 0.214 and -0.382 , and the correlation coefficients with SI were 0.246 and -0.297 . Specifically, the Rsc exhibited a strong correlation with SI, indicating that changes in light intensity directly influenced participants' physiological responses. Weak correlations were also observed between the Rsc and T_a , T_g , and T_{mrt} . Additionally, linear regression analysis revealed a positive correlation between the Rsc and participants' visual-thermal sensations—particularly with the TSV and, to a lesser extent, with the SSV. This suggests that both thermal and non-thermal effects directly impact individuals' perceptions and lead to physiological reactions. For example, higher T_a results in a sensation of heat, triggering sweating and blood vessel dilation, which leads to an increased Rsc.

Conversely, high SI induces tension and the constriction of blood vessels via visual stimulation, resulting in an elevated Rsc. In contrast, T_a , T_g , and T_{mrt} have weaker effects on the Rsc, suggesting that their influence on human comfort occurs indirectly and may depend on overall environmental conditions and interactions. For example, high T_g may contribute to discomfort in the human body, but this discomfort may be caused by a combination of multiple thermal effect factors rather than by temperature alone. Conversely, the nSCR exhibited a significant negative correlation with T_a , T_g , T_{mrt} , and SVF and a significant positive correlation with R_h , while showing relatively weak correlations with Mws, the UTCI, and SI. Linear regression analysis demonstrated negative correlations between the nSCR and the TSV—and especially between the nSCR and the SSV—indicating that the nSCR is particularly sensitive to changes in light intensity. The weak relationship between the nSCR and the TSV may be attributed to the limits of thermal sensations' influence on physiological and psychological activation states or the limited range of changes in thermal sensations accounted for by the experiment.

The study also revealed that the Rsc had a stronger positive correlation with SI in environments with lower T_a , while the nSCR exhibited a more pronounced negative correlation with T_a in environments with lower SI. The correlation coefficients for the Rsc between the SSV and TSV were 0.81 and 0.57, respectively, while the correlation coefficients for the nSCR between the SSV and TSV were 0.78 and 0.68, respectively. The Rsc's higher correlation with the TSV suggests that it is a more reliable predictor of thermal sensation. Conversely, the nSCR was more strongly correlated with the SSV, indicating that it can be used to accurately predict visual comfort. Therefore, it may be concluded that the Rsc can predict the TSV under intense stress (UTCI: 26–32), while the nSCR can be employed to predict the SSV under even greater stress (UTCI: 32–38).

Furthermore, SCR did not exhibit significant correlations with environmental variables, and spatial differences had minimal effects. Therefore, SCR should be regarded as a

supplemental indicator for evaluating thermal comfort. Linear regression analysis revealed negative correlations between SCR and the TSV, as well as SCR and the SSV, suggesting that environmental stimuli have a substantial impact on SCR. While environmental variables primarily affect visual–thermal comfort, their effects on physiological responses, such as blood circulation and sweat gland secretion, may not be immediately reflected in SCR measurements. This likely explains the weak correlation between SCR and environmental variables, as well as the minor effects different spaces had on this index. However, SCR still has value for its ability to provide supplementary information on visual–thermal comfort and indicates specific points on the human body that allow the effects of outdoor environmental stimuli to be accurately evaluated.

The findings of this study have important implications for landscape planning, design, and the sustainable development of thermal environments on campuses in China. Despite certain limitations, the experiment highlighted the influence of spatial characteristics on the visual–thermal comfort of its participants. Campus planners and landscape designers should consider how to effectively combine landscape elements and spatial layout in ways that improve overall visual and thermal comfort. The correlations between visual comfort, thermal comfort, and human physiological parameters (such as skin conductance) identified in this study can also be used as a basis for evaluating human experience and satisfaction. It should be noted that, as this study focused on a specific campus setting under typical summer weather conditions, future research should attempt to explore the relationships between a wider range of physiological parameters over multiple seasons, providing a more comprehensive understanding of visual–thermal comfort in green campus spaces.

5. Conclusions

This research offers valuable information and references for the visual–thermal aspects of environmental planning and the sustainable development of landscapes on Chinese campuses. Although subject to certain limitations, the experiment underscores the impact of spatial characteristics on participants' visual–thermal comfort. Campus planners and landscape designers should carefully consider how to effectively integrate landscape elements and spatial layouts to enhance overall visual and thermal comfort. The observed correlations between visual comfort, thermal comfort, and physiological parameters such as skin conductance can provide a foundation for evaluating human experiences and satisfaction. Specifically, this study provides the following conclusions and optimization strategies for green space design:

- (1) Even under the same climatic conditions, each space exhibits different microclimates and visual environmental characteristics, resulting in significant differences in environmental parameters such as T_a and SI . Within the same type of space, areas with dense vegetation and water features tend to have lower T_a and higher R_h . Therefore, designing green spaces with different vegetation densities and waterfront features can create diverse microclimates and visual environments and address environmental challenges. For example, in areas with pronounced urban heat island effects, increasing vegetation coverage and incorporating water elements help to lower temperatures and provide people with more comfortable and diverse thermal and visual experiences.
- (2) There is a significant correlation between the thermal comfort and visual comfort experienced in outdoor blue–green spaces. Environmental parameters such as T_a , R_h , W_s , T_{mrt} , and SI influence people's perceptions and sensations of the outdoor environment, thereby affecting their visual–thermal comfort levels. The results of this study indicate that T_a , R_h , and T_{mrt} are related to thermal comfort, while SI and SVF are related to visual comfort. Therefore, when designing green spaces, it is crucial to consider how to optimize thermal and visual comfort. Adjusting environmental parameters such as temperature, humidity, wind speed, radiant temperature, and lighting can contribute to the enhancement of the thermal and visual experience. The thoughtful planning of green space layouts should consider the unique characteristics

and functional needs of different spaces to ensure a range of comfortable thermal and visual experiences. For instance, incorporating structures that provide shade and offer cool resting areas while maintaining unobstructed views can enhance the overall comfort of an outdoor environment, especially in hot weather conditions.

- (3) Physiological parameters vary with visual stimuli and microclimate conditions, reflecting their association with visual–thermal comfort. We used linear regression analysis to examine the relationships between three physiological parameters (Rsc, SCR, and nSCR), a thermal sensation vote (TSV), and a sunlight sensation vote (SSV). The results indicated that the Rsc is positively correlated with the TSV and the SSV, with R^2 values of 0.8101 and 0.576, respectively. SCR is negatively correlated with TSV and SSV, with R^2 values of 0.8749 and 0.828, respectively. Our comprehensive analysis of physiological parameters (such as skin conductance) and perceptual data offers valuable insights into physiological responses to various environmental conditions, guiding landscape design and providing a path for enhancing and optimizing thermal and visual comfort levels in outdoor landscapes.

Our study focused on visual–thermal comfort in a specific campus environment during the summer. Future research should explore a broader range of physiological parameters across different seasons to enhance our understanding of visual–thermal comfort in green campus spaces. Additionally, considering the influence of climatic conditions, further investigation is needed to explore the correlation between thermal and visual comfort in diverse environmental contexts. Strengthening the analysis of physiological parameters using larger sample sizes and controlled experimental conditions will improve the reliability of our findings. This research contributes to designing comfortable and sustainable outdoor spaces.

Author Contributions: Conceptualization, X.W. and Z.C.; data curation, Z.C. and D.M.; formal analysis, X.W. and J.C.; funding acquisition, X.W. and X.J.; investigation, Z.C. and T.Z.; methodology, X.W.; project administration, D.M. and X.J.; resources, J.C. and X.J.; software, Z.C. and D.M.; supervision, J.C. and X.J.; validation, X.W., Z.C. and D.M.; visualization, Z.C. and T.Z.; writing—original draft, X.W. and Z.C.; writing—review and editing, X.W., Z.C. and J.C. All authors have read and agreed to the published version of the manuscript.

Funding: This research was funded by the Science and Technology Program of Guangzhou, China, grant number 202102010438, presided by Xuefei Wang, including four members, and the Science and Technology Program of Guangzhou University, China, grant number PT252022006.

Institutional Review Board Statement: The study was conducted in accordance with the Declaration of Helsinki and approved by the Ethics Committee of the College of Architecture and Urban Planning, Guangzhou University.

Informed Consent Statement: Informed consent was obtained from all subjects involved in the study.

Data Availability Statement: The datasets generated during or analyzed during the current study are available from the corresponding author on reasonable request.

Conflicts of Interest: The authors declare neither conflict of interest nor competing interests.

Abbreviations

BMI, Body mass index; Clo, clothing; EDA, electrodermal activity; HSV, humidity sensation vote; Met, metabolic rate; Mws, moving wind speed; nSCR, number of skin conductance responses; Rh, relative humidity; RSV, solar radiation sensation vote; SC, skin conductance; SCR, skin conductance response; SI, sunlight intensity; SPV, sunlight preference vote; SSV, sunlight sensation vote; SVF, sky view factor; Ta, air temperature; TCV, thermal comfort vote; Tg, globe temperature; Tmrt, mean radiant temperature; TPV, thermal preference vote; TSV, thermal sensation vote; UTCI, universal thermal comfort index; VCV, visual comfort vote; Ws, wind speed; WSV, wind sensation vote.

References

1. Ebi, K.L.; Bowen, K. Green and blue spaces: Crucial for healthy, sustainable urban futures. *Lancet* **2023**, *401*, 529–530. [[CrossRef](#)]
2. Zhou, L.; Shen, G.; Woodfin, T.; Chen, T.; Song, K. Ecological and economic impacts of green roofs and permeable pavements at the city level: The case of Corvallis, Oregon. *J. Environ. Plan. Manag.* **2018**, *61*, 430–450. [[CrossRef](#)]
3. Lin, T.P.; Tsai, K.T.; Hwang, R.L.; Matzarakis, A. Quantification of the effect of thermal indices and sky view factor on park attendance. *Landsc. Urban Plan.* **2012**, *107*, 137–146. [[CrossRef](#)]
4. Louafi, S.; Abdou, S.; Reiter, S. Effect of vegetation cover on thermal and visual comfort of pedestrians in urban spaces in hot and dry climate. *Nat. Technol.* **2017**, *17*, 30–42.
5. Yan, T.; Jin, Y.; Jin, H. Combined effects of the visual-thermal environment on the subjective evaluation of urban pedestrian streets in severely cold regions of China. *Build. Environ.* **2023**, *228*, 109895. [[CrossRef](#)]
6. Lam, C.K.C.; Yang, H.; Yang, X.; Liu, J.; Ou, C.; Cui, S.; Kong, X.; Hang, J. Cross-modal effects of thermal and visual conditions on outdoor thermal and visual comfort perception. *Build. Environ.* **2020**, *186*, 107297. [[CrossRef](#)]
7. Lam, C.K.C.; Weng, J.; Liu, K.; Hang, J. The effects of shading devices on outdoor thermal and visual comfort in Southern China during summer. *Build. Environ.* **2023**, *228*, 109743. [[CrossRef](#)]
8. *Standard 55-2004; Thermal Environmental Conditions for Human Occupancy*. ANSI/ASHRAE: Atlanta, GA, USA, 2004.
9. Sodoudi, S.; Zhang, H.; Chi, X.; Müller, F. The influence of spatial configuration of green areas on microclimate and thermal comfort. *Urban For. Urban Green.* **2018**, *34*, 85–96. [[CrossRef](#)]
10. Lai, D.; Liu, W.; Gan, T.; Liu, K.; Chen, Q. A review of mitigating strategies to improve the thermal environment and thermal comfort in urban outdoor spaces. *Sci. Total. Environ.* **2019**, *661*, 337–353. [[CrossRef](#)]
11. Haupt, C.; Huber, A.B. How axons see their way—Axonal guidance in the visual system. *Front. Biosci. Landmark* **2008**, *13*, 3136–3149. [[CrossRef](#)]
12. *EN12665; Light and Lighting—Basic Terms and Criteria for Specifying Lighting Requirements*. European Committee for Standardization: Brussels, Belgium, 2018.
13. Yang, W.; Moon, H.J. Cross-modal effects of illuminance and room temperature on indoor environmental perception. *Build. Environ.* **2018**, *146*, 280–288. [[CrossRef](#)]
14. Zhang, T.; Hong, B.; Su, X.; Li, Y.; Song, L. Effects of tree seasonal characteristics on thermal-visual perception and thermal comfort. *Build. Environ.* **2022**, *212*, 108793. [[CrossRef](#)]
15. Chen, T.; Pan, H.; Lu, M.; Hang, J.; Lam, C.K.C.; Yuan, C.; Pearlmutter, D. Effects of tree plantings and aspect ratios on pedestrian visual and thermal comfort using scaled outdoor experiments. *Sci. Total. Environ.* **2021**, *801*, 149527. [[CrossRef](#)] [[PubMed](#)]
16. Te Kulve, M.; Schlangen, L.; van Marken Lichtenbelt, W. Interactions between the perception of light and temperature. *Indoor Air* **2018**, *28*, 881–891. [[CrossRef](#)]
17. Lau, K.K.L.; Choi, C.Y. The influence of perceived aesthetic and acoustic quality on outdoor thermal comfort in urban environment. *Build. Environ.* **2021**, *206*, 108333. [[CrossRef](#)]
18. Narimani, N.; Karimi, A.; Brown, R.D. Effects of street orientation and tree species thermal comfort within urban canyons in a hot, dry climate. *Ecol. Inform.* **2022**, *69*, 101671. [[CrossRef](#)]
19. Zhuang, D.; Zhang, X.; Lu, Y.; Wang, C.; Jin, X.; Zhou, X.; Shi, X. A performance data integrated BIM framework for building life-cycle energy efficiency and environmental optimization design. *Autom. Constr.* **2021**, *127*, 103712. [[CrossRef](#)]
20. Chinazzo, G.; Wienold, J.; Andersen, M. Daylight affects human thermal perception. *Sci. Rep.* **2019**, *9*, 13690. [[CrossRef](#)]
21. Kulve, M.T.; Schlangen, L.; Schellen, L.; Souman, J.L.; Lichtenbelt, W.V.M. Correlated colour temperature of morning light influences alertness and body temperature. *Physiol. Behav.* **2018**, *185*, 1–13. [[CrossRef](#)]
22. Liu, W.-W.; Lian, Z.-W.; Deng, Q.; Rong, W.-F. Objective evaluation indices of human thermal comfort. *J. Cent. South Univ. (Sci. Technol.)* **2011**, *42*, 521–526.
23. Persiani, S.G.L.; Kobas, B.; Koth, S.C.; Auer, T. Biometric Data as Real-Time Measure of Physiological Reactions to Environmental Stimuli in the Built Environment. *Energies* **2021**, *14*, 232. [[CrossRef](#)]
24. Pan, J.; Li, N.; Zhang, W.; He, Y.; Hu, X. Investigation based on physiological parameters of human thermal sensation and comfort zone on indoor solar radiation conditions in summer. *Build. Environ.* **2022**, *226*, 109780. [[CrossRef](#)]
25. Liu, B.; Lian, Z.; Brown, R.D. Effect of Landscape Microclimates on Thermal Comfort and Physiological Wellbeing. *Sustainability* **2019**, *11*, 5387. [[CrossRef](#)]
26. Kim, S.; Yun, B.Y.; Choi, J.Y.; Kim, Y.U.; Kim, S. Quantification of visual thermal perception changes in a wooden interior environment using physiological responses and immersive virtual environment. *Build. Environ.* **2023**, *240*, 110420. [[CrossRef](#)]
27. Van, B.W. Visual, biological and emotional aspects of lighting: Recent new findings and their meaning for lighting practice. *Leukos* **2005**, *2*, 7–11.
28. Luo, W.; Kramer, R.; Kompier, M.; Smolders, K.; de Kort, Y.; Lichtenbelt, W.V.M. Effects of correlated color temperature of light on thermal comfort, thermophysiology and cognitive performance. *Build. Environ.* **2023**, *231*, 109944. [[CrossRef](#)]
29. Mansi, S.A.; Barone, G.; Forzano, C.; Pigliautile, I.; Ferrara, M.; Pisello, A.L.; Arnesano, M. Measuring human physiological indices for thermal comfort assessment through wearable devices: A review. *Measurement* **2021**, *183*, 109872. [[CrossRef](#)]
30. Takakura, J.; Nishimura, T.; Choi, D.; Egashira, Y.; Watanuki, S. Nonthermal sensory input and altered human thermoregulation: Effects of visual information depicting hot or cold environments. *Int. J. Biometeorol.* **2015**, *59*, 1453–1460. [[CrossRef](#)]

31. Zhu, R.; Zhang, X.; Yang, L.; Liu, Y.; Cong, Y.; Gao, W. Correlation analysis of thermal comfort and physiological responses under different microclimates of urban park. *Case Stud. Therm. Eng.* **2022**, *34*, 102044. [[CrossRef](#)]
32. Lin, Y.; Yang, L.; Chai, X. Prediction of thermal comfort voting based on psycho-physiological adaptation. *J. HV&AC* **2021**, *51*, 111–117.
33. Sharma, M.; Kacker, S.; Sharma, M. A brief introduction and review on galvanic skin response. *Int. J. Med. Res. Health Sci.* **2016**, *2*, 13–17. [[CrossRef](#)]
34. Jukiewicz, M.; Łupkowski, P.; Majchrowski, R.; Marcinkowska, J.; Ratajczyk, D. Electrodermal and thermal measurement of users' emotional reaction for a visual stimuli. *Case Stud. Therm. Eng.* **2021**, *27*, 101303. [[CrossRef](#)]
35. Liu, N.; Qin, Y. *Building Thermal Environment*; Tsinghua University Press: Beijing, China, 2005.
36. Ye, H.; Zhu, X. Study on the Effect of Spatial Characteristics and Health Restoration of Urban Parks in Harbin City in Autumn—Taking Zhaolin Park as an Example. *J. Hum. Settl. West China* **2018**, *33*, 73–79.
37. *ISO7243: 2017; Ergonomics of the Thermal Environment—Assessment of Heat Stress Using the WBGT (Wet Bulb Globe Temperature) Index*. ISO: Geneva, Switzerland, 2017.
38. *ISO 7726: 1998; Ergonomics of the Thermal Environment: Instruments for Measuring Physical Quantities*. ISO: Geneva, Switzerland, 1998.
39. *GB/T 5700-2008; Measurement Methods for Lighting*. China Architecture & Building Press: Beijing, China; pp. 6–82013.
40. Mayes, H.S.; Navarro, M.; Satchell, L.P.; Tipton, M.J.; Ando, S.; Costello, J.T. The effects of manipulating the visual environment on thermal perception: A structured narrative review. *J. Therm. Biol.* **2023**, *112*, 103488. [[CrossRef](#)] [[PubMed](#)]
41. *ISO7730-2005; Moderate Thermal Environments-Determination of the PMV and PPD Indices and Specification of the Conditions for Thermal Comfort*. International Organization for Standardization: Geneva, Switzerland, 2005.
42. Braithwaite, J.J.; Watson, D.G.; Jones, R.; Rowe, M. A guide for analyzing electrodermal activity (EDA) & skin conductance re-sponses (SCRs) for psychological experiments. *Psychophysiology* **2013**, *49*, 1017–1034.
43. Doberenz, S.; Roth, W.T.; Wollburg, E.; Maslowski, N.I.; Kim, S. Methodological considerations in ambulatory skin conductance monitoring. *Int. J. Psychophysiol.* **2011**, *80*, 87–95. [[CrossRef](#)]
44. Jin, H.; Luo, C.; Jin, H. The influence of urban park's visible green index on human physical and mental health: A case study of Hangzhou city. *South Archit.* **2022**, *212*, 43–51.
45. Christopoulos, G.I.; Uy, M.A.; Yap, W.J. The Body and the Brain: Measuring Skin Conductance Responses to Understand the Emotional Experience. *Organ. Res. Methods* **2019**, *22*, 394–420. [[CrossRef](#)]
46. Van Dooren, M.; Janssen, J.H. Emotional sweating across the body: Comparing 16 different skin conductance measurement locations. *Physiol. Behav.* **2012**, *106*, 298–304. [[CrossRef](#)]
47. Matzarakis, A.; Rutz, F.; Mayer, H. Modelling radiation fluxes in simple and complex environments—Application of the RayMan model. *Int. J. Biometeorol.* **2007**, *51*, 323–334. [[CrossRef](#)]
48. Geng, Y.; Hong, B.; Du, M.; Yuan, T.; Wang, Y. Combined effects of visual-acoustic-thermal comfort in campus open spaces: A pilot study in China's cold region. *Build. Environ.* **2022**, *209*, 108658. [[CrossRef](#)]

Disclaimer/Publisher's Note: The statements, opinions and data contained in all publications are solely those of the individual author(s) and contributor(s) and not of MDPI and/or the editor(s). MDPI and/or the editor(s) disclaim responsibility for any injury to people or property resulting from any ideas, methods, instructions or products referred to in the content.